Fault Detection and Diagnosis for a Nonlinear Hydraulic Actuator

IOP Conf. Series: Materials Science and Engineering **575** (2019) 012014 doi:10.1088/1757-899X/575/1/012014

Fault Detection and Diagnosis for a Nonlinear Hydraulic Actuator

Juan Felipe Ortiz, Carlos Borrás and Diego Sepulveda

Mechanical Engineering Faculty, Universidad Industrial de Santander, 680003 Bucaramanga, Colombia

juanfortiz60@gmail.com; juan2168908@correo.uis.edu.co

Abstract. In this work a nonlinear dynamic and mathematic model for the position control of a hydraulic actuator with internal leakage was developed, simulations were made and a basic PID control in order to check the actuator behaviour. An internal leakage emulator was installed bypassing the two chambers of the hydraulic cylinder. Time and position data were acquired via Quanser Q8-USB and saved for modelling and validation purposes, sinusoidal and square signals and both for four fault conditions. Data were classified through MATLAB Simulink algorithm having in consideration parity equations and residual generation, obtaining a high level of validation for the proposed model and the desired responses and fault detection, diagnosis and classification.

1. Introduction

Hydraulic actuators are widely used in industrial applications due to their excellent power-size relation, their capacity to apply high forces indefinitely and their high response [1]. Hydraulic servo systems combine the advantages of hydraulic actuators with the versatility of electronics to give the most powerful actuators in modern industrial applications like robotics, aerospace industry, mining, testing equipment and production lines [2] [3].

However, electrohydraulic actuators exhibit a highly and complex nonlinear dynamic performance [4] [5]. The main nonlinearities are due to compressibility of the hydraulic fluid, the flow-pressure relationship in the servo valve, friction forces and internal and external leakage in the actuator [6] [7].
In this work a nonlinear mathematic and dynamic model was first developed having in consideration the internal leakages through the two chambers of the hydraulic actuator. Experimental validation was made in Dynamics and Structural Control Lab at Universidad Industrial de Santander in order to check the accuracy of the dynamic model. Fault detection was made with the residual generated between the two models and fault classification and diagnosis was carried out with features extraction having in consideration the residual and internal leakage flow in order to create boundaries to successfully classify the case studies.

2. Nonlinear Dynamic Model

The schematic representation of the system under consideration is shown in figure 1. The hydraulic actuator is double rod and is commanded by a servo valve. The objective is tracking precisely a specified displacement trajectory.

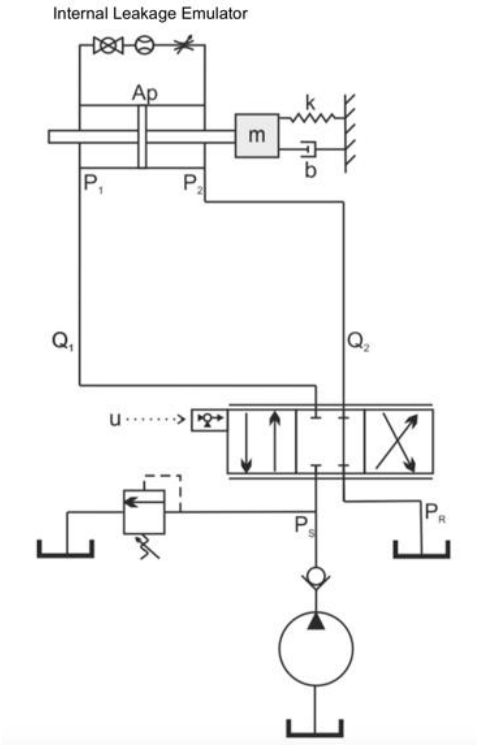

Figure 1. Hydraulic system schematic.

2.1. Actuator Analysis

The motion dynamics of the mass of the actuator is obtained applying Newton's second law:

$$m\ddot{x}_p = A_p P_L - b\dot{x}_p - kx_p \tag{1}$$

where m, b and k are the mass, the viscous damping coefficient and the mass stiffness. x_p is the actuator's displacement, A_p the effective annular piston area and P_L the load pressure, defined as $P_L = P_1 - P_2$.The actuator's dynamics is obtained by applying the continuity principle:

$$Q_L = A_p\dot{x}_p + \frac{V_t}{4\beta}\dot{P}_L \tag{2}$$

where β is the effective bulk modulus, V_t the total fluid volume trapped in the actuator's chambers and system's pipes, Q_{leak} is the leakage flow between the two chambers and Q_L is the flow supplied by the servo valve to move the load, defined as.

$$Q_L = Q_{Leak} + \frac{Q_1 + Q_2}{2} \tag{3}$$

2.2. Servo valve Analysis

The flow supplied by the servo valve is related with the spool displacement by the following equation, assuming that the orifices are symmetric:

$$Q_L = C_d w x_v \sqrt{\frac{P_S - P_L}{\rho}} \tag{4}$$

where C_d is the discharge coefficient through the orifice, w is the area gradient of the orifice, x_v is the spool displacement, P_S is the supply pressure y ρ is the hydraulic fluid density. The relationship between control voltage and spool displacement is obtained:

$$u = \frac{1}{k_v} x_v \tag{5}$$

$$x_v = u k_{ev} \tag{6}$$

where k_v is the gain of the servo valve, and u the control voltage.

Combining equations, flow equation remains:

$$Q_L = u k_v C_d w \sqrt{\frac{P_S - P_L}{\rho}} \tag{7}$$

2.3. Nonlinear Dynamic Model Without Fault

Using equations 1, 2, 3, 4, 5 and assuming that $Q_{Leak} = 0$, the nonlinear dynamic model without fault are constructed as follows:

$$\ddot{x}_p = \frac{1}{m}\left[A_p P_L - b\dot{x}_p - k x_p\right] \tag{8}$$

$$\dot{P}_L = \frac{4\beta}{V_t}\left[u k_v C_d \omega \sqrt{\frac{P_S - P_L}{\rho}} - A_p \dot{x}_p\right] \tag{9}$$

The nonlinear plant without fault is built using these nonlinear equations 8 and 9 and is shown in Figure 2. The input to the plant is the servo valve voltage u and the output is the actuator's position x_p which completes the feedback look of the system.

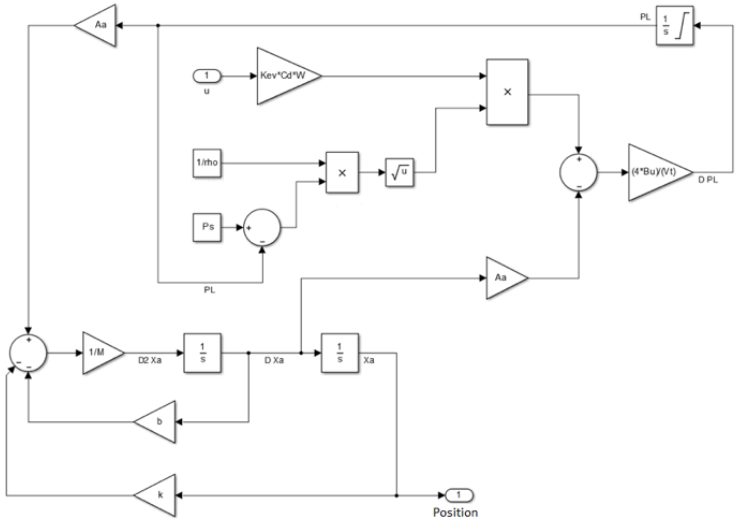

Figure 2. Nonlinear model subplant without fault modelled in Simulink.

2.4. Nonlinear Dynamic Model Without Fault

Using equations 1, 2, 3, 4, 5 and having in consideration the internal leakage inside the actuator, the nonlinear dynamic model with fault are constructed as follows:

$$\dot{P}_L = \frac{4\beta}{V_t}\left[Q_L - Q_{leak} - A_p\dot{x}_p\right] \tag{10}$$

O According to Sepehri [8], the internal leakage flow can be model as:

$$Q_{leak} = C_{leak}w_{leak}\sqrt{\frac{2P_L}{\rho}} \tag{11}$$

where C_{leak} is the flow through a hole coefficient and C_{leak} is the leakage area. Through mathematical operations, the main equations are:

$$\ddot{x}_p = \frac{1}{m}\left[A_pP_L - b\dot{x}_p - kx_p\right] \tag{12}$$

$$\dot{P}_L = \frac{4\beta}{V_t}\left[uk_vC_d\omega\sqrt{\frac{P_S - P_L}{\rho}} - C_{leak}w_{leak}\sqrt{\frac{2P_L}{\rho}} - A_p\dot{x}_p\right] \tag{13}$$

The nonlinear plant with fault is built using the equations 12 and 13 and is shown in Figure 3. The input to the plant is the servo valve voltage u and the output is the actuator's position x_p which completes the feedback look of the system.

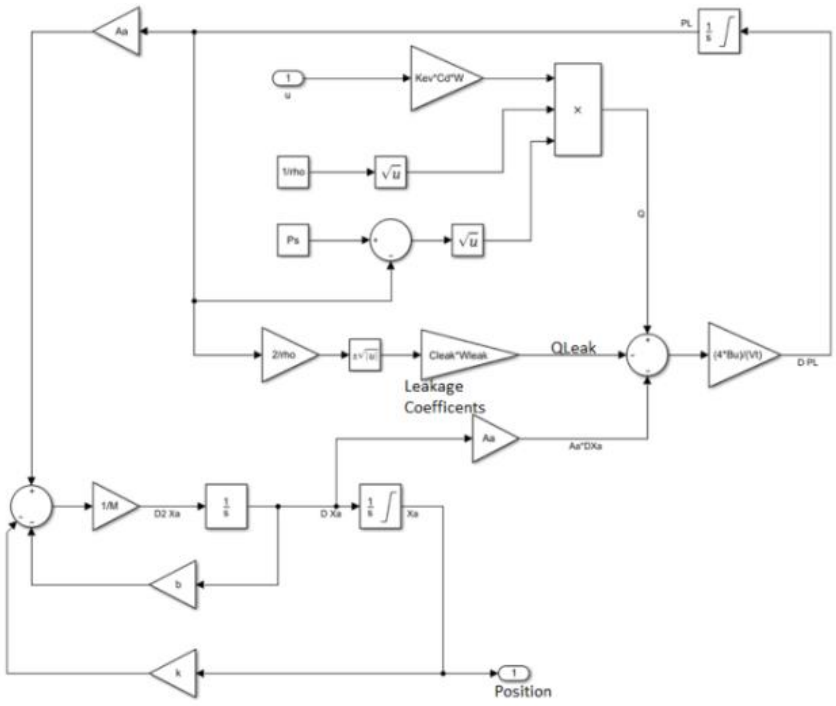

Figure 3. Nonlinear model subplant with fault modelled in Simulink.

3. Simulation

The simulations of the position of the hydraulic actuator were carried out using two types of signal inputs: sine and square wave. For both signals the position set-point was 0.15 [m], which is the half of the actuator's stroke.

Simulations were made through computerized software (MATLAB and Simulink). Faulty and nonfaulty models were analysed and compared using parity equations in order to generate a residual for fault detection, evaluation and classification.

3.1. Normal system simulation

In this case, the Simulink nonlinear dynamic model without fault shown in Figure 2 are used. The physical values and constants were used from a Karpenko and Sepehri [8] research and are listed in Table 1 in order to verify the model behaviour, but in this case, $w_{leak} = 0$

3.2. Faulty system simulation

In this case, the Simulink nonlinear dynamic model with fault shown in Figure 3 are used. The physical values and constants were used from a Karpenko and Sepehri [8] research and are listed in Table 1 in order to verify the model behaviour. In this case, $w_{leak} = 5e^{-7}\ \frac{mm^2}{mm}$ so that the fault can be noticed.

3.3. Systems comparison

For fault detection and diagnosis, is important to compare the system behaviour in both scenarios. This simulation integrates the two previous models in which flow and position data were compared to generate a residual that is essential for a correct fault detection and diagnosis

The position error or residual are generated by the following equation and Simulink block model were made and represented in Figure 4:

$$r'(s) = [GP(s) - GM(s)]u(s) \tag{14}$$

Table 1. Constants and physical values for modelling without fault.

Parameter	Symbol	Nominal Value	Units
Supply pressure	Ps	17,2	Mpa
Total mass of piston, rods and load	m	12	Kg
Viscous damping coefficient	b	1000	$\frac{N\ s}{m}$
Load spring constant	k	75	$\frac{kN}{m}$
Piston annulus area	A	633	mm^2
Cylinder volume	V	468	mm^3
Leakage orifice coefficient of discharge	Cleak	0,7	--
Leakage orifice area	Wleak	5e-07	$\frac{mm^2}{mm}$
Hydraulic fluid density	ρ	847	$\frac{Kg}{m^3}$
Effective bulk modulus	Bu	689	Mpa
Servo valve coefficient of discharge	Cd	0,6	--
Servo valve orifice area gradient	w	20,75	$\frac{mm^2}{mm}$
Servo valve spool position gain	Kev	0,0406	$\frac{mm}{V}$

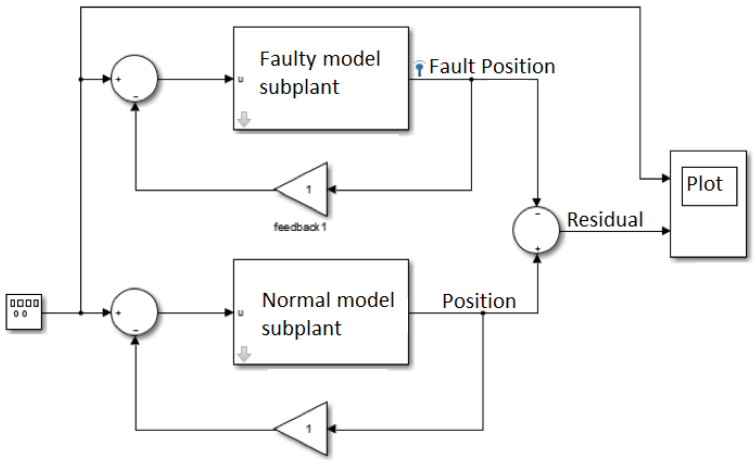

Figure 4. Simulink blocks model comparing the faulty and nonfaulty model for residual generation.

Figure 5 shows the position of both models with a sine signal as input, and the residual generated having in consideration the equation 14.

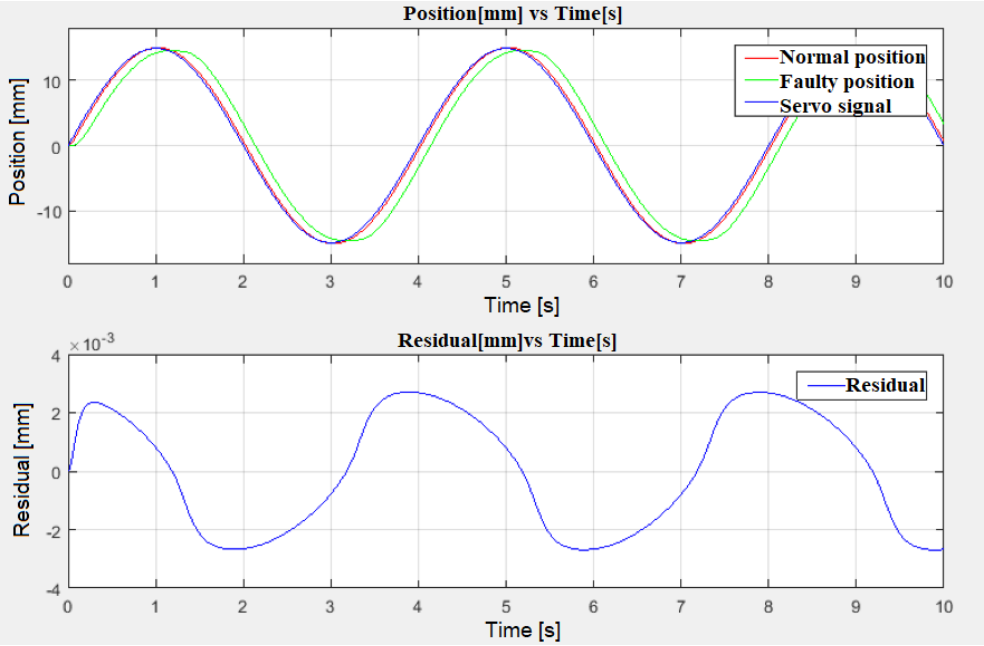

Figure 5. Residual obtained from the faulty and nonfaulty model comparison for sine wave input.

In both cases, the fault is noticeable, the hydraulic actuator can't reach the set point and presents a delay with the input signal. The residual shows a disturbance and error between the two signals and shows an evident fault.

4. Experimental Model Validation

The validation was done in the hydraulic uniaxial seismic shake table of the Dynamics and Structural Control Lab at Universidad Industrial de Santander (shown in Figure 7). The seismic table consists of a Parker hydraulic cylinder, a MOOG 76-263 servo valve, Quanser Q8 USB data acquisition and MTS

hydraulic unit and complementary equipment to carry out the assembly of the hydraulic uniaxial seismic shake table shown in Figure 6.

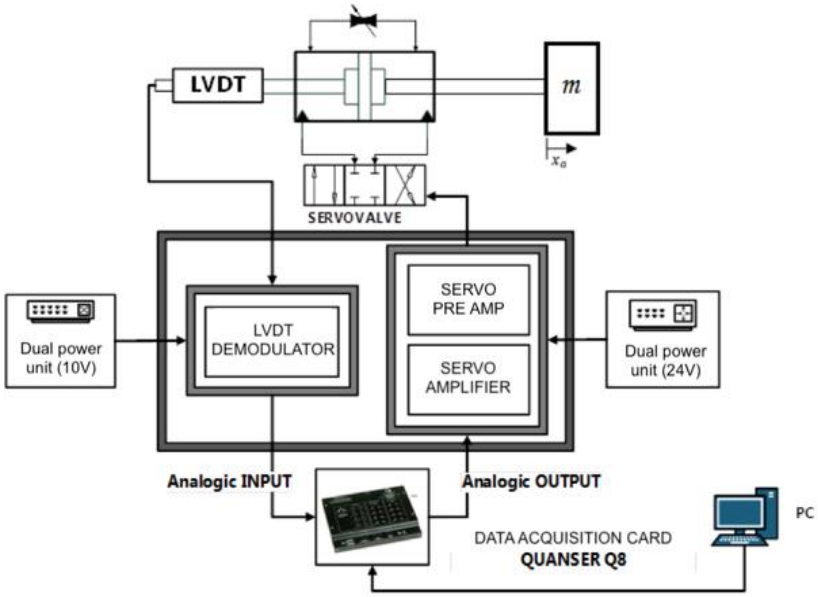

Figure 6. Schematic of hydraulic and electric assembly used to set up the hydraulic uniaxial seismic shake unit and achieve the experimental data acquisition.

Figure 7. Experimental assembly of the hydraulic uniaxial seismic shake table.

4.1. Data acquisition

Data acquisition were made in groups of five vectors, for a 4-inch amplitude and frequency of 0,1Hz, 1Hz and 10Hz both for a square and sinusoidal input signal. The five vectors were averaged to reduce possible errors.

4.2. Validation

The MATLAB and Simulink nonlinear model was calibrated with the real parameters of the experimental assembly with the purpose of have a computational model which can simulate the real assembly with minimal error. These parameters are shown in the Table 2.

Table 2. Constants and physical values for modelling without fault.

Parameter	Symbol	*Nominal Value*	Units
Mass	M	85	Kg
Stroke	Cc	0,1524	m
Active area	Aa	$1{,}62e^{-3}$	m^2
Total volume	Vt	Aa*Cc	m^3
Supply pressure	Ps	$6{,}2e^{6}$	PSI

For the validation, three different methods were used to confirm the accuracy of the simulation model developed.

The Determination Coefficient: It makes several observations of the variable to be predicted and the variances of the residual and the dependent variable are related.

$$\boldsymbol{\rho^2} = 1 - \frac{\sigma_{res}}{\sigma_{dep}} \tag{15}$$

where σ_{res} is the residual variance and σ_{dep} is the dependent variable variance, in this case the experimental data.

The Correlation Coefficient: It is a measure that aims to quantify the degree of relationship and joint variation between two variables, is a statistical measure that quantifies the linear dependence between two variables.

$$\boldsymbol{R} = \frac{Cov(obs,mod)}{Std(obs)*Std(mod)} \tag{16}$$

where $Cov(obs, mod)$ is the covariance between the model and experimental data, $Std(obs)$ is the standard deviation of experimental data and $Std(mod)$ the standard deviation of the model data.

The Coefficient of Correlation of Concordance: It throws the degree of reproducibility between the data measured in the test bench and the outputs generated by the model.

$$\boldsymbol{CCC} = \frac{A^2+B^2-C^2}{A^2+B^2+D^2} \tag{17}$$

where A and B are the simulation variances and measure data, C is the residual variance and D the average difference between measures.

The absolute error of this case is 0,845%, $\boldsymbol{\rho^2}$ coefficient is 99,94%, $\boldsymbol{R}$ coefficient is 99,97 and $\boldsymbol{CCC}$ coefficient 99,96%. That indicates that the computational model for this case of study describes satisfactorily the real behaviour of the experimental assembly with very small errors.

5. Fault Detection and Classification

Internal leakage was simulated through a needle valve in bypass between the two chambers. The position data were taken in groups of five vectors and for four cases of valve opening (0%, 33,33%, 66,66% and 100%) for a 4-inch amplitude and frequency of 0,1Hz, 1Hz and 10Hz both for a square and sinusoidal input signal. The five vectors were averaged to reduce possible errors.

Figure 8 shows the position of a 0,1Hz sine signal with the four cases of study (without fault, slight fault, medium fault and critical fault).

As expected, the previous image shows that the response of the system varies according to the opening level of the needle valve which, in this specific case, is simulating an internal leakage failure in the actuator.

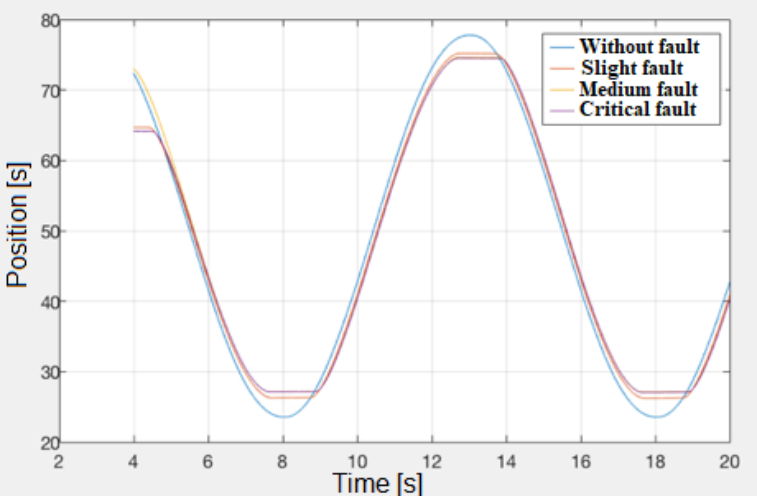

Figure 8. Position data simulation results for 0.1Hz sine wave input with four internal leakage scenarios.

5.1. Classification ranges

According to Watton and Pham [9], A severe failure in the piston seal of a hydraulic cylinder can pass more than 30% of the flow intended by the servo valve for work. Therefore, it will become the point of reference to generate the fault classification ranges.

Using the simulation previously validated with the sample taken, the percentage of opening of the simulated needle valve was manually set so that it would pass 30% of the work flow, as Watton suggests, the system flows are shown in Figure 9.

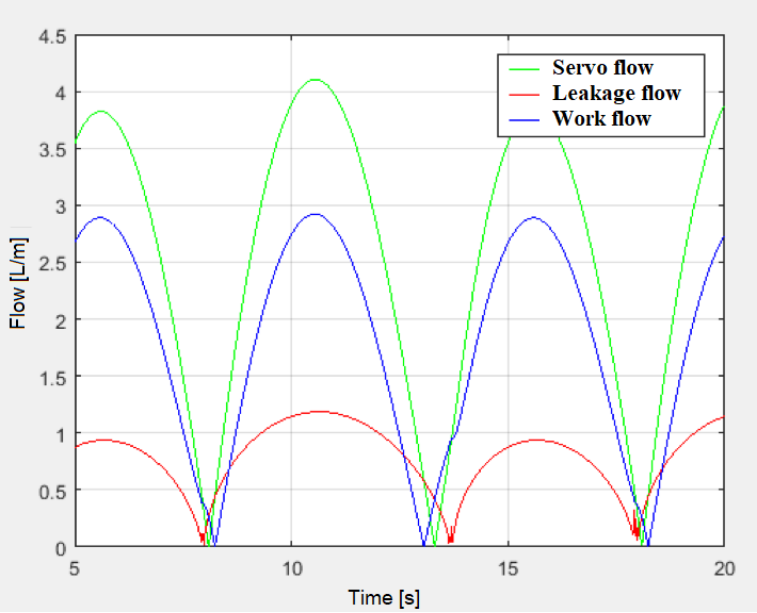

Figure 9. System flows simulation results for 0.1Hz sine wave input when internal leakage is greater than 30% of the work flow.

In addition, the points were searched where 20% and 10% of the flow are lost respectively to classify in three fault levels. Repeating this procedure for the different configurations and having in consideration the fault ranges, Table 3 shows the different flow constants calculated for every scenario.

Table 3. Cleak coefficient for different fault scenarios

Fault	QLeak	0.1 Hz Sqr	0.1 Hz Sin	1 Hz Sqr	1 Hz Sin	10 Hz Sqr	10 Hz Sin
Normal	0	0,1	0,015	0,001	0,001	0,001	0,001
Slight	10%	0,25	0,15	0,35	0,3	0,25	0,12
Medium	20%	0,5	0,35	0,8	0,6	0,7	0,23
Critical	30%	0,85	0,6	1,2	0,9	0,85	0,35
Super	50%	1,4	1,35	2,5	1,9	1,3	0,65

5.2. Fault classification

Considering the classification ranges, a feature extraction of the position signal (Mean, RMS and Standard Deviation) was carried out to improve the accuracy of the classification algorithm hence these values are significantly affected by internal leakage, frequency and type of the signal and they maintain intervals of considerable size, a clear tendency and they remain on the same quadrant.

Fault detection and classification algorithm analyse the residual between the two signals, and compare the flow and features extracted in order to cluster and locate each signal in a classification range generating an output message or alert.

Figure 10 shows how far the cylinder stroke is influenced under the presence of a fault that causes a loss of flow in the piston, from values lower than 10% to 30% and supercritical of 50%.

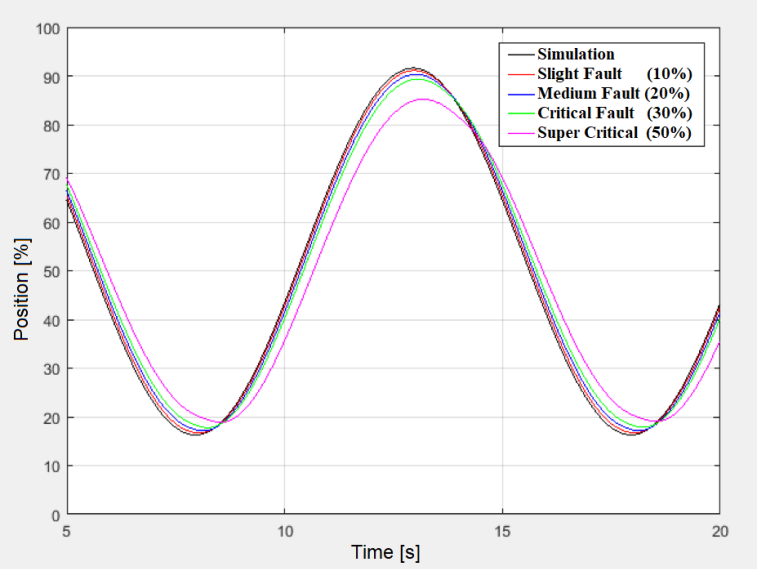

Figure 10. Position simulation results in four fault scenarios (0%, 10%, 20%,30% and 50% of internal leakage) for 0.1Hz sine wave.

Figure 11 shows how the flows behave, according to the simulation, during the test, you can see how the flow sent by the servo valve must be increasing to compensate the loss, but also the work flow is reduced with the increase of the loss flow.

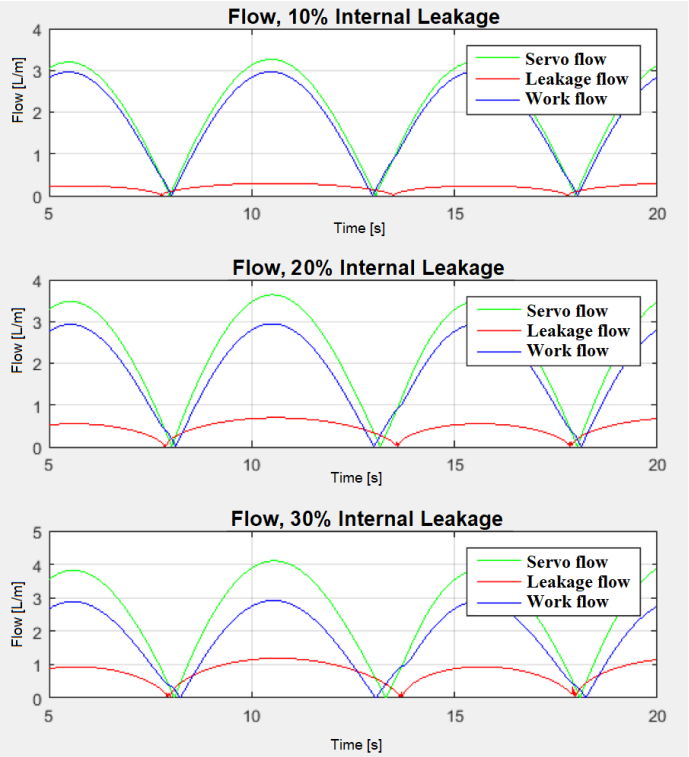

Figure 11. Flows data simulation results for 0.1Hz sine wave input with three internal leakage fault scenarios (10%, 20% and 30% of internal leakage).

Table 4 shows the Leakage coefficient, the flows and the features extracted with the limit values for the clustering and diagnosis.

Table 4. Parameters for fault clustering

Fault	C Leak	Q Servo [L/m]	Q Leak [L/m]	Mean	RMS	Std
Normal	0,015	1,9148	0,0018	0,0215	0,0269	0,0162
Slight	0,15	2,0887	0,2044	0,0508	0,0554	0,022
Medium	0,35	2,3151	0,4709	0,1171	0,1263	0,0472
Critical	0,6	2,5484	0,7797	0,2015	0,2163	0,0788
Super	1,35	3,319	1,6704	0,4186	0,4525	0,172

Having in consideration Table 4, the data previously acquired were passed through the MATLAB fault detection and diagnosis algorithm which process de data and classify successfully all the cases of study (0,1Hz, 1Hz and 10Hz for sine and square wave)

6. Conclusions

- In this work the non-linear dynamic and mathematical model of a hydraulic seismic shake table with and without internal leakage through the two chambers of the actuator was developed.
- Simulations were carried out for sine and square wave as input signal with frequencies of 0,1Hz, 1Hz and 10Hz and validated with experimental data, having correlation coefficients higher than 96% and errors lower than 1%. Fault detection were developed through parity equations and residual analysis of the system.

- Three classification ranges were stablished: Slight fault (0-10% leakage flow) medium fault (10%-20% leakage flow) critical fault (20%-30% leakage flow) and super critical fault (higher than 30% of leakage flow) having in consideration as a several failures the internal leakage higher than 30%.
- Fault diagnosis and classification was realized through MATLAB algorithm which extract important features of the signal and clusters in the four classification ranges for each case of study with 94,4% of accuracy.

7. Observations

Future work will include another fault detection and identification techniques as Artificial Neural Networks and Fault Tolerance.

8. References

[1] F. Basile, P. Chiacchio, and D. Del Grosso. International Journal of Robotics and Automation, 24(1):20–37, 2009
[2] Rolf. Isermann. Fault Diagnosis Aplications. Editorial Springer.350 p.
[3] C. Borrás, J. L. Sarmiento, J. F. Ortiz. ASME, 1 (2018)
[4] Y. Jianyong., Y. GUICHAO, and M. Dawei. 2014. Research Article. School of Mechanical Engineering, Nanjing University of Science and Technology, Nanjing 210094, China. 39.
[5] C. Borrás, J. L. Sarmiento, J. F. Ortiz, XI Congreso Colombiano de Métodos Numéricos, 6, 9 (2017)
[6] Michael G. Skarpetis, Fotis N. Koumboulis, and Achilleas S. Ntellis. 2014 22nd Mediterranean Conference on Control and Automation (MED), (6):1553–1558, 2014.
[7] Hong Ming Chen, Jyh Chyang Renn, and Juhng Perng Su. International Journal of Advanced Manufacturing Technology, 26(1-2):117– 123, 2005
[8] Mark Karpenko and Nariman Sepehri. Journal of Dynamic Systems, Measurement, and Control, 132(5):054505–1 – 054505–7, 2010.
[9] Le, T. T., Watton, J., and Pham, D. T., 1997, Proceedings of The Institute of Mechanical Engineers, Part I, journal of Systems and Control Engineering, 211, pp. 307–317

Acknowledgements

The authors of this work thank the Universidad Industrial de Santander, the Faculty of Physical - Mechanical Engineering and the Mechanical Engineering School for the funding and support.